

Supplementary Material

Dual-functional lactic acid/zinc chloride deep eutectic solvent pretreatment: simultaneous production of antioxidative lignin and high-performance hard carbon anodes for sodium-ion batteries

Yuan Pan ^{a, c, d}, Xuefeng Yao ^b, Rongjun Li ^{a, c, d}, Wen Zhang ^b, Fang Gu ^{b, c, d*},
Mingqiang Zhu ^{a, b, c, d*}

^a College of Forestry, Northwest Agriculture & Forestry University, Yangling 712100,
China.

^b College of Mechanical and Electronic Engineering, Northwest Agriculture & Forestry
University, Yangling 712100, China.

^c Key Laboratory of *Eucommia* of National Forestry and Grassland Administration,
Yangling 712100, China.

^d Key Laboratory of Shaanxi Province on Development and Utilization of Economic
Plant Resources, Yangling 712100, China.

Corresponding author's e-mail address: zmqsx@nwsuaf.edu.cn (M. Q. Zhu),
gufang@nwafu.edu.cn (F. Gu)

2. Materials and methods

2.1 Correlated calculations

The lignin recovery and the delignification ratio: The DES treatment performance analysis equations are as follows,

$$\text{Lignin recovery (\%)} = \frac{\text{Lignin recovered in residue after pre}}{\text{Initial amount of lignin in raw m}}$$

$$\text{Delignification ratio (\%)} = (1 - \text{Lignin recovery}) \times 100\% \#(2)$$

The crystallinity index (CrI): The calculation was based on the XRD patterns of solid substrates according to the following equation,¹

$$C_r I (\%) = \frac{I_{200} - I_{AM}}{I_{200}} \times 100\% \#(3)$$

The intensity of (200) peak (I_{200}) located between the scattering angles of $2\theta=22^\circ$ to 23° represented the sum of the crystalline and amorphous components, while the minimal diffraction intensity near 18° between the (110) and (200) peaks reflected the proportion of the amorphous content (I_{AM}).

The $d_{(002)}$ value: The average interlayer d-spacing could be conducted according to Bragg's equation,

$$2d \sin \theta = n\lambda \#(4)$$

where d is the average interlayer spacing, 2θ is the diffraction angle, λ is the wavelength of the incident X-ray excitation beam, n is the order of reflection.

The layer stacking distance (L_c) and the longitudinal dimension (L_a): The calculation was based on the XRD patterns of the hard carbons were calculated according to the formula (Scherrer equation),

$$La \& Lc = \frac{\kappa\lambda}{\beta \cos \theta} \#(5)$$

In this formula, κ is Scherrer constant (κ is 0.9 for Lc and κ is 1.84 for La), λ is the radiation wavelength, β is the half-height width of the (002) peak, θ is the reflection angle of (002) or (100).

The inhibition percentage (IP, %) of the DPPH radical: The calculation was based on the following equation, and the relationship between IP and concentration of lignin could be obtained. The concentration of the lignin at 50% IP is IC_{50} and the radical scavenging index (RSI) is the inverse of IC_{50} .

$$IP (\%) = \frac{A_0 - A_t}{A_0} \times 100\% \#(6)$$

Diffusion coefficient of sodium ion (D_{Na^+}): The diffusion coefficient of sodium-ion (D_{Na^+}) was estimated by the Fick's second law equation,

$$D = \frac{4}{\pi\tau} \left(\frac{m_B V_M}{M_B S} \right)^2 \left(\frac{\Delta E S}{\Delta E \tau} \right)^2 \#(7)$$

In which τ represents the pulse duration, m_B and S are related with the active mass loading and surface area of the electrode, V_M and M_B refer to the molar volume and weight of the active material, and (refer to voltage variation leaded by galvanostatic charge/discharge and pulse, respectively) can be acquired from the GITT curves.

The techno-economic assessment of producing lignin and EUWCs: Equipment cost was estimated based on a combination of vender quotes and literature sources,^{2, 3} and capital cost was estimated for all major technical components and processes within the plant using the Lang Factor method. The total cost was determined by method in previous reported study. In the base case, it was assumed that the instrument was 10

years with a discount rate of 5%, and an once production yield of 2.5 kg of high-performance carbon material (Table S9). The instrument depreciation price was obtained by the followed equation,

$$\text{Instrument depreciation price} = \frac{(1 - \text{Estimated net salvage value}) \times \text{Equipment price}}{\text{Expected service life} \times 12}$$

2.2 Determination of the content of lignin Ph–OH Groups

The phenolic hydroxyl (Ph–OH) group content in lignin fractions was quantified using the FC (Foline–Phenol) method with guaiacol as the standard.⁴ In detail, 2 mL of the 1 N FC reagent was added to 1 mL lignin solution (0.5 mg/mL) with reacting for 5 min at room temperature. After reaction, 45 mL of deionized water and 2 mL of 20% (w/v) sodium carbonate solution were added. Then, the mixture was stirred with 3 h, and the absorbance of samples was measured at 760 nm by spectrophotometer (Mapada UV-vis TU-1880, China). All measurements were carried out in triplicate with the relative deviations of <5%.⁵

2.3 Free radical scavenging activity of lignin

The antioxidant activity of lignin fractions was determined by using 1,1-diphenyl-2-picrylhydrazyl (DPPH) radicals.⁶ Specifically, a series of lignin in dioxane-water (9/1, v/v) with concentrations ranging from 0.01 to 0.1 mg/mL was prepared.⁶ For the assay, 0.64 mL of each sample was mixed with 2.36 mL of 24.5 mg/L DPPH methanol solution. The reaction was allowed to proceed in the dark at 25 °C for 16 min. The scavenging activity was determined by monitoring the absorbance of DPPH solution at 515 nm immediately (A_0) and after 16 min (A_t) using an ultraviolet/visible

spectrophotometer.

2.4 Lignin purity determination

The purity of the regenerated lignin was defined as the mass percentage of lignin in the total recovered solids. The carbohydrate components of lignin were analyzed by NREL protocol. Sulphuric acid (72%, w/w) was used for acid hydrolysis of the biomass sample for 1 h at 30 °C in a water bath. Then, the acid hydrolysed sample was diluted to 4% acid concentration and kept in an autoclave at 121°C for 1 h. The sample was cooled to room temperature and vacuum-filtered using a filtration crucible. The carbohydrate components were determined by HPIC. Ash content was determined in the muffle furnace at 575 °C for 24 h. The elemental composition of the regenerated lignin was analyzed using energy-dispersive X-ray spectroscopy (EDS) attached to a scanning electron microscope. The element quantification of samples was analyzed by elemental analyzer (EURO EA 3000, Italy). The lignin purity was calculated as the following,

$$\text{Lignin purity (\%)} = 100\% - (\text{total carbohydrates wt\%} + \text{ash wt\%}) \quad (9)$$

2.5 DFT calculations

The relevant calculations were carried out with the Gaussian 16 program package. The β -O-4 type lignin dimer model and the LA/ZnCl₂/DES configuration were globally searched using the Molclus program,⁷ followed by geometry optimization and frequency analysis at the M06-2X/6-311G (d, p) level with GD3 dispersion correction. The binding energy between the lignin dimer and the LA/ZnCl₂ cluster was calculated as the following,

$$\Delta E = E_{Lignin-DES} - (E_{Lignin} + E_{DES}) \#(10)$$

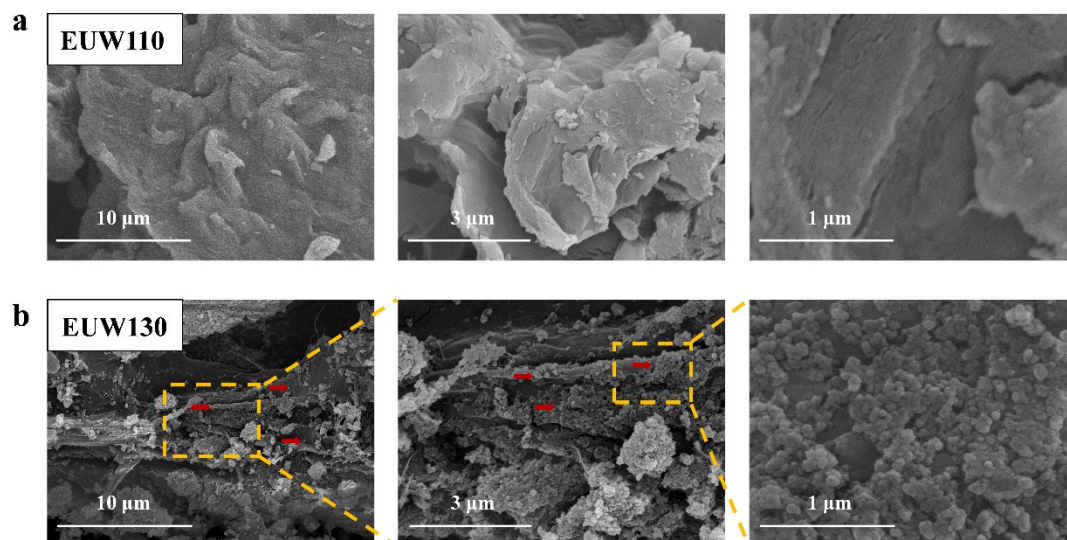


Fig. S1. SEM images of the solid residues after DES pretreatment at (a) 110 °C and (b) 130 °C (magnification 15.0 k \times , 35.0 k \times , 50.0 k \times).

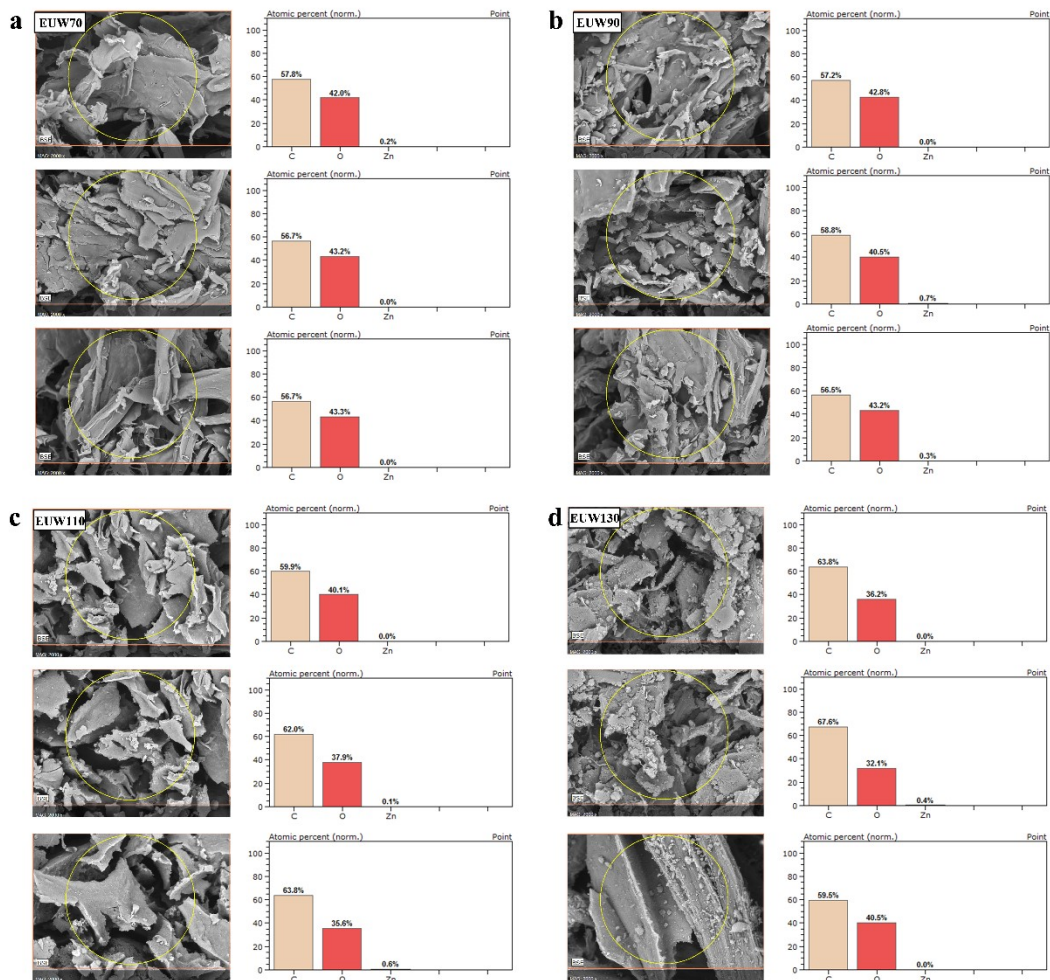


Fig. S2. SEM images and EDS results of the solid residues after DES pretreatment at (a) 70 °C, (b) 90 °C, (c) 110 °C and (d) 130 °C.

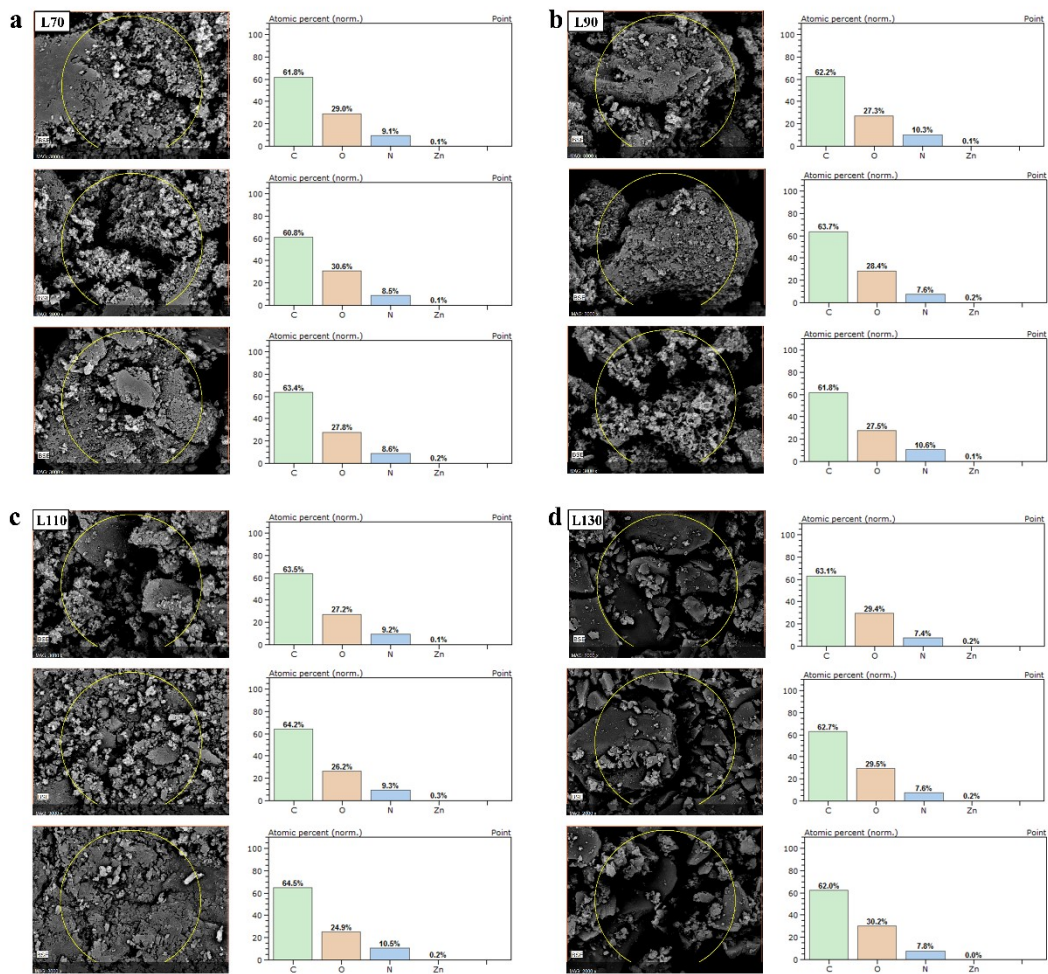


Fig. S3. SEM images and EDS results of lignin.

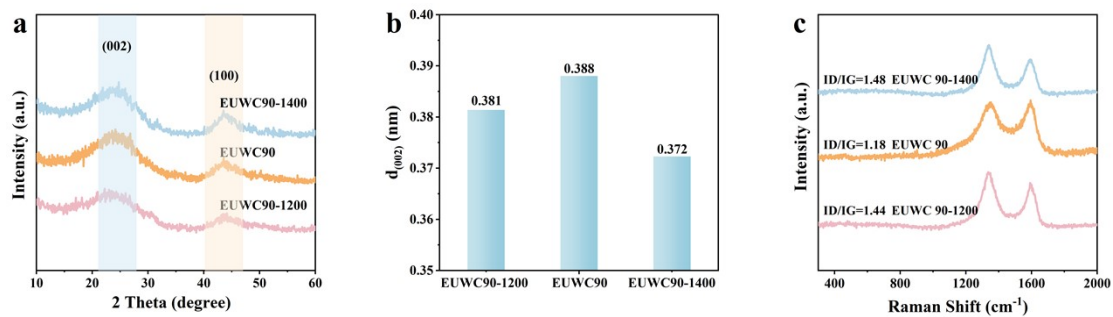


Fig. S4. (a) XRD spectra, (b) $d_{(002)}$, (c) Raman spectra of EUWC90-1200, EUWC90 and EUWC90-1400.

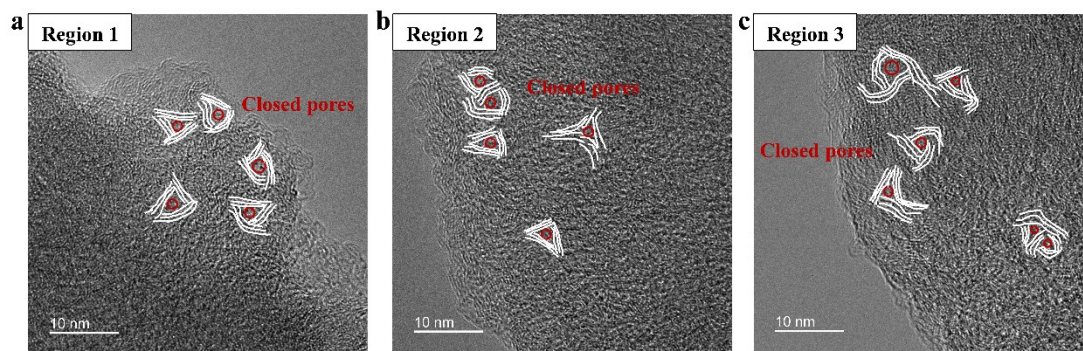


Fig. S5. HRTEM images of EUWC90 acquired from different regions.

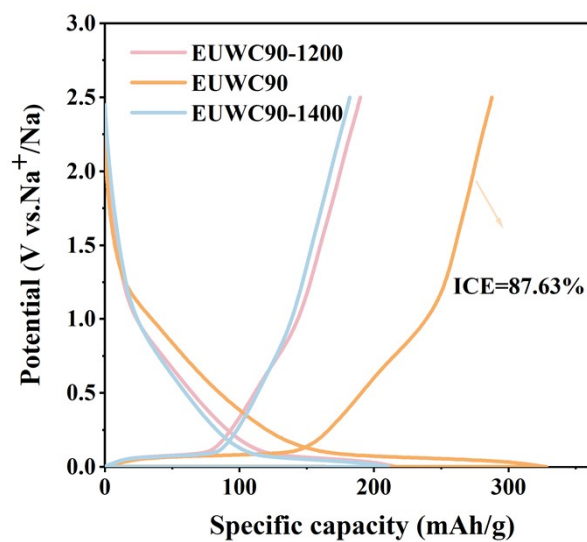


Fig. S6. The first charge/discharge curves of EUWC90-1200, EUWC90 and EUWC90-1400.

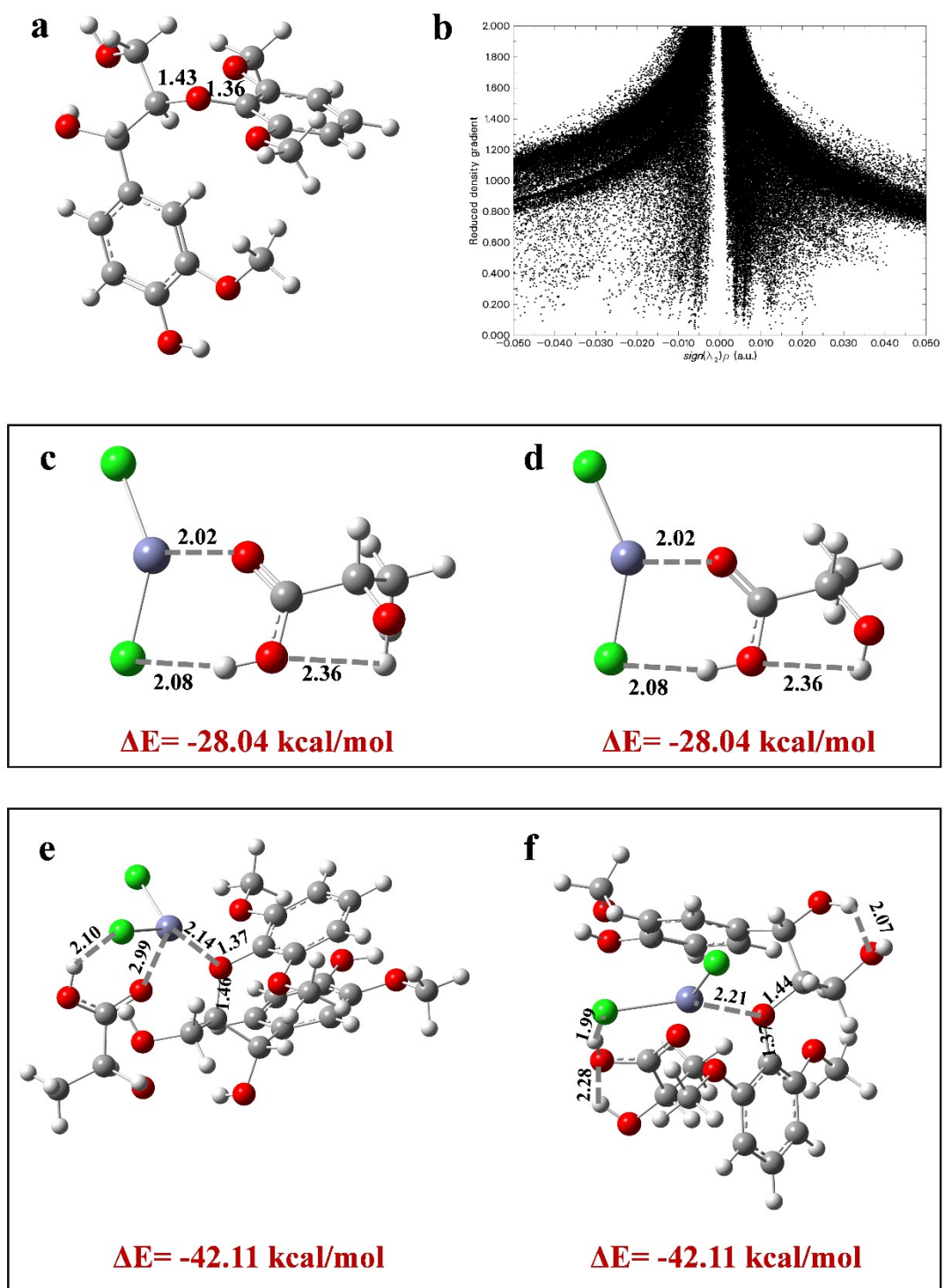


Fig. S7. (a) Chemical structure of the β-O-4-type lignin dimer model compound, (b) 2D RDG analysis of electron density of ZnCl₂/LA/lignin, (c) and (d) relative energies and bond lengths of optimized structures of ZnCl₂-LA, (e) and (f) Relative energies and bond lengths of optimized structures of ZnCl₂-LA and lignin dimer.

Table S1. The treatment efficiency of DES on EUW and chemical composition of EUWs.

Samples	Delignification (%)	Lignin yield (%)	Chemical composition (%)		
			Cellulose	Hemicellulose	Lignin
EUW	-	-	19.71	7.08	24.67
EUW70	69.23±0.15	57.13±0.27	41.21	4.42	17.60
EUW90	89.03±0.69	78.67±0.66	53.02	4.37	7.17
EUW110	94.99±0.26	91.65±0.34	68.78	3.18	2.20
EUW130	42.48±0.30	24.53±0.47	25.39	0.25	41.60

Table S2. The recovery rate and pretreatment efficiency of DES in five cycles of pretreatment on EUW at 110 °C for 3 h.

Cycle numbers	DES recovery (%)	Delignification (%)	Lignin yield (%)
1	89.72±0.23	94.65±0.72	92.00±0.52
2	88.36±0.14	92.13±0.32	89.72±0.46
3	87.64±0.30	88.35±0.29	85.25±0.33
4	86.50±0.37	85.30±0.48	82.30±0.39
5	87.26±0.17	85.12±0.46	82.13±0.62

Table S3. The carbohydrates analysis and ash content in regenerated lignin (%).

Samples	Ara	Gal	Glu	Xyl	Man	Ash	Total
L70	ND ^a	0.14±0.01	0.26±0.02	0.07±0.02	ND	0.33±0.03	0.80±0.08
L90	ND	ND	0.06±0.01	ND	ND	0.42±0.06	0.50±0.07
L110	ND	0.05±0.01	ND	ND	ND	0.13±0.01	0.18±0.02
L130	ND	0.06±0.01	ND	ND	ND	0.19±0.03	0.25±0.04

^aND: not detected.

Ara: Arabinose, Gal: Galactose, Glu: Glucose, Xyl: Xylose, Man: Mannose.

Table S4. The element quantification of lignin.

Samples	C (%)	H (%)	O (%)	N (%)
MWL	55.25	5.96	37.37	1.42
L70	59.20	5.57	34.59	0.68
L90	60.10	5.46	33.94	0.51
L110	62.50	5.33	31.76	0.42
L130	63.60	5.15	31.02	0.20

Table S5. Assignments of main ^{13}C - ^1H cross signals in 2D-HSQC NMR spectra of lignin fractions.

Label	$\delta_{\text{C}}/\delta_{\text{H}}$ (ppm)	Assignments
B_{β}	53.2/3.06	C_{β} - H_{β} in β - β (resinol) substructures (B)
OCH_3	56.2/3.70	C-H in methoxyls (OMe)
A_{γ}	59.7/3.34-3.82	C_{γ} - H_{γ} in c-hydroxylated β - O -4' substructures (A)
A'_{γ}	63.2/4.35	C_{γ} - H_{γ} in γ -acylated β - O -4' substructures (A')
C_{γ}	62.0/3.76	C_{γ} - H_{γ} in β - β' resinol substructures (C)
B_{γ}	71.2/3.72-4.18	C_{γ} - H_{γ} in β - β resinol substructures (B)
A_{α}	71.9/4.81	C_{α} - H_{α} in β - O -4' substructures (A)
$\text{S}_{2,6}$	103.6/6.71	$\text{C}_{2,6}$ - $\text{H}_{2,6}$ in syringyl units (S)
$\text{S}'_{2,6}$	106.5/7.34	$\text{C}_{2,6}$ - $\text{H}_{2,6}$ in oxidized S units (S')
G_2	110.6/6.98	C_2 - H_2 in guaiacyl units (G)
G_5	114.4/6.72	C_5 - H_5 in guaiacyl units (G)
G_6	119.2/6.76	C_6 - H_6 in guaiacyl units (G)

Table S6. The weight-average (M_w), number-average (M_n) molecular weights, polymer dispersion index (PDI), phenolic hydroxyl content (Ph-OH) and free radical scavenging index (RSI) of DES lignin samples.

DES Lignin	Mw (g/mol)	Mn (g/mol)	PDI	Ph-OH (mmol/g)	RSI
L70	3890	2050	1.90	1.77±0.08	7.00±0.23
L90	3750	1970	1.90	1.87±0.03	9.47±0.07
L110	3750	1520	2.47	2.29±0.06	13.79±0.03
L130	2760	1620	1.70	2.22±0.06	13.38±0.08

Table S7. The element quantification of EUWs.

Samples	C (%)	H (%)	O (%)	N (%)
EUW	45.99	5.67	48.08	0.26
EUW70	43.67	6.00	50.30	0.03
EUW90	44.65	6.19	49.16	0.00
EUW110	43.81	6.10	50.09	0.00
EUW130	61.73	5.02	33.11	0.14

Table S8. Physical parameters of the samples from XRD for EUWCs.

Samples	$2\theta_{(002)}$	d_{002} (nm)	La (nm)	Lc (nm)	Highly disordered (%)	Pseudo-graphitic (%)	Graphite-like (%)
EUWC	25.24	0.353	3.01	1.72	34.15	33.33	32.52
EUWC70	24.22	0.367	2.30	1.51	25.68	28.38	45.94
EUWC90	22.84	0.389	1.97	1.57	25.92	34.96	39.12
EUWC110	22.89	0.388	1.92	1.43	29.09	30.64	40.27
EUWC130	23.80	0.373	1.56	0.94	36.56	33.33	30.11

Table S9. Physical parameters of the samples from XPS C1s for EUWCs.

Samples	C (%)	O (%)	sp ² /sp ³	C=O/C-O
EUWC	96.47	3.53	3.66	1.05
EUWC70	91.18	8.82	3.96	1.07
EUWC90	86.67	13.34	7.42	1.55
EUWC110	87.27	12.73	5.52	1.20
EUWC130	91.31	8.69	5.13	1.14

Table S10. The galvanostatic charge/discharge capacity and ICE of EUWCs at a current rate of 20 mA g⁻¹.

Samples	Initial discharge capacity (mAh g ⁻¹)	Initial charge capacity (mAh g ⁻¹)	ICE (%)
EUWC	134.1	105.2	78.5
EUWC70	303.4	269.6	88.9
EUWC90	328.3	287.7	87.6
EUWC110	278.2	260.5	93.6
EUWC130	202.8	171.2	84.4

Table S11. The galvanostatic charge/discharge capacity and ICE of EUWC90-1200, and EUWC90-1400 at a current rate of 20 mA g⁻¹.

Samples	Initial discharge capacity (mAh g ⁻¹)	Initial charge capacity (mAh g ⁻¹)	ICE (%)
EUWC90-1200	216.2	189.9	87.8
EUWC90-1400	210.8	182.0	86.3

Table S12. The electricity consumption and material use for preparing lignin and EUWCs and charge-discharge.

Item	Raw	DES treatment
EUW (g)	20	20
LA (g)	-	322
ZnCl ₂ (g)	-	78
DES treatment time (h)	-	3
The power for DES treatment (kW)	-	26.13
50% ethanol (L)	-	1.2
Stirring time (h)	-	1.5
The power of stirring (kW)	-	0.009
Pyrolysis time (h)	2	2
The power of pyrolysis (kW)	1.5	1.5
N ₂ (L)	5	5
HCl (mL)	5	5
Distilled water (mL)	56.5	99.4
Stirring time (h)	1	1.75
Crushing time (h)	0.5	0.5
The power of cushing (kW)	2	2
Drying time (h)	12	12
The power of drying (kW)	1	1
Charge-discharge time (h)	10.17	30.97
The power of charge-discharge (kW)	0.6	0.6

Table S13. The price and cost of electricity and material.

Item	Raw	DES treatment
EUW (yuan/g)	0.012	0.012
EUW (yuan)	0.240	0.240
LA price (yuan/g)	-	0.050
ZnCl ₂ price (yuan/g)	-	0.056
LA/ZnCl ₂ cost (yuan)	-	16.537
50% ethanol price (yuan/L)	-	9.000
50% ethanol cost (yuan)	-	10.800
N ₂ price (yuan/L)	0.024	0.024
N ₂ cost (yuan)	0.120	0.120
HCl price (yuan/mL)	0.021	0.021
HCl cost (yuan)	0.105	0.105
Distilled water price (yuan/mL)	2.000	2.000
Distilled water cost (yuan)	113.000	198.800
Electricity consumption (kWh)	22.110	86.860
Electricity price (yuan/kWh)	0.725	0.725
Instrument depreciation price (yuan)	0.582	0.774

References

- 1 K. S. Salem, N. K. Kasera, M. A. Rahman, H. Jameel, Y. Habibi, S. J. Eichhorn, A. D. French, L. Pal and L. A. Lucia, *Chem. Soc. Rev.*, 2023, **52**, 6417-6446.
- 2 X. Mao, Y. Li, X. Hu, R. Tian and W. Yu, *Appl. Energy*, 2023, **338**, 120929.
- 3 J. Mi, X.-R. Wang, R.-J. Fan, W.-H. Qu and W.-C. Li, *Energy Fuels*, 2012, **26**, 5321-5329.
- 4 E. A. Ainsworth and K. M. Gillespie, *Nat. Protoc.*, 2007, **2**, 875-877.
- 5 Z. Li, J. Zhang, L. Qn and Y. Ge, *ACS Sustainable Chem. Eng.*, 2018, **6**, 2591-2595.
- 6 T. Dizhbite, G. Telysheva, V. Jurkjane and U. Viesturs, *Bioresour. Technol.*, 2004, **95**, 309-317.
- 7 T. Lu, *Molclus program, Version 1.10*, 2023, <https://www.keinsci.com/research/molclus.html> (accessed 2026-04-15).